Journal of Plant Physiology 169 (2012) 1329–1339

Contents lists available at SciVerse ScienceDirect

Journal of Plant Physiology

journal homepage: www.elsevier.de/jplph

Hsp90 binds microtubules and is involved in the reorganization of the microtubular network in angiosperms

Jana Krtková [a,*], Aleksandra Zimmermann [b], Kateřina Schwarzerová [a], Peter Nick [b]

[a] Department of Experimental Plant Biology, Faculty of Science, Charles University in Prague, Viničná 5, 128 44 Prague 2, Czech Republic
[b] Institute of Botany 1 and Center for Functional Nanostructures (CFN), University of Karlsruhe, Kaiserstraße 2, D-76128 Karlsruhe, Germany

ARTICLE INFO

Article history:
Received 2 April 2012
Received in revised form 14 June 2012
Accepted 15 June 2012

Keywords:
Cold
Heat-shock protein 90
Microtubules
Tobacco
Tubulin

ABSTRACT

Microtubules (MTs) are essential for many processes in plant cells. MT-associated proteins (MAPs) influence MT polymerization dynamics and enable them to perform their functions. The molecular chaperone Hsp90 has been shown to associate with MTs in animal and plant cells. However, the role of Hsp90–MT binding in plants has not yet been investigated. Here, we show that Hsp90 associates with cortical MTs in tobacco cells and decorates MTs in the phragmoplast. Further, we show that tobacco Hsp90_MT binds directly to polymerized MTs *in vitro*. The inhibition of Hsp90 by geldanamycin (GDA) severely impairs MT re-assembly after cold-induced de-polymerization. Our results indicate that the plant Hsp90 interaction with MTs plays a key role in cellular events, where MT re-organization is needed.

Introduction

Microtubules (MTs) are highly dynamic polymers that are essential for cell growth, morphogenesis, development and signaling of plant cells (for a review, see Lloyd and Chan, 2004). During the plant cell cycle, MTs form characteristic arrays that are organized by dynamic disassembly and re-assembly of MTs in combination with movements of polymers. The microtubular dynamics are regulated by several specific microtubule-associated proteins (MAPs, for a recent review on plant MAPs see Hamada, 2007). In addition to dynamics, severing, and sliding of microtubular polymers, specific MAPs mediate the interaction of MTs with cellular compartments or organelles. The interaction of interphasic cortical MTs with the plasma membrane, for example, is mediated by phospholipase D (Gardiner et al., 2001), and the endoplasmic reticulum is co-aligned with MTs by formin FH4, suggesting a further role of FH4 at the interface of the actin and microtubular cytoskeleton (Deeks et al., 2010). In addition to a group of MT-binding proteins highly conserved in all eukaryotic cells, some binding proteins differ considerably between plant and non-plant cells, correlating with specific functions of plant MTs. Interestingly, the affinity of binding proteins is not very pronounced in many cases. It can be regulated by oligomerization, as shown for plant katanin (Stoppin-Mellet et al., 2007), or by interaction with other binding proteins, as found for the so-called +TIPs, i.e. the complex at the growing MT plus-end that regulates the microtubular elongation process (for a recent review, see Akhmanova and Steinmetz, 2008). The highly dynamic and combinatorial activity of some plant MAPs renders functional analysis difficult, because proteins that do not show pronounced affinity and/or specificity *in vitro* can act *in vivo* in concert with other proteins as specific key regulators. Such proteins that are sufficiently plastic to interact with several substrates are nevertheless expected to be very important for the control of plant MTs organization. In fact, the plant chaperone CCT (Nick et al., 2000), and heat-shock protein 90 (Freudenreich and Nick, 1998; Petrasek et al., 1998) were shown to interact with MTs in addition to other MT-independent functions.

Hsp90 is a highly conserved molecular chaperone essential for protein folding and stability in eukaryotic cells. In animals, many Hsp90 substrates, including proteins, involved in signal transduction and cell development have been described (Wegele et al., 2004). In plants, Hsp90 is essential for the stress response triggered by resistance proteins (R-proteins, Boter et al., 2007; Takahashi et al., 2003), and is involved in MAP kinase cascades (Takabatake et al., 2007). Since Hsp90 predominantly mediates the shift of regulatory and signaling proteins between active and inactive states (Rutherford and Zuker, 1994), it acts at the interface of several developmental pathways (Rutherford and Lindquist, 1998).

Among other proteins, the cytoskeletal proteins actin and tubulin have been reported as interactors of Hsp90 (Koyasu et al., 1986; Sanchez et al., 1988; Wegele et al., 2004). The interaction of Hsp90 with MTs seems to play an important role in eukaryotic cells, and its

Abbreviations: EPC, ethyl-N-phenylcarbamate; GDA, geldanamycin; MAP, microtubule-associated protein; MT, microtubule; PPB, preprophase band.

* Corresponding author. Tel.: +420 221 951 689; fax: +420 221 951 704.
E-mail address: akcni.krtecek@post.cz (J. Krtková).

0176-1617/$ – see front matter © 2012 Elsevier GmbH. All rights reserved.
http://dx.doi.org/10.1016/j.jplph.2012.06.010

functional importance is illustrated by a growing body of evidence in animal cells. The interaction of Hsp90 with MTs is very complex and occurs at least at four levels in animals. Hsp90 interacts with tubulin dimers in animal cells (Sanchez et al., 1988; Weis et al., 2010) as well as with assembled MTs (Fostinis et al., 1992; Williams and Nelsen, 1997). Hsp90 is also a part of the heterocomplex associating with MTs during nuclear transport of steroid hormones (Harrell et al., 2002; Pratt et al., 1999), and strikingly, Hsp90 is a core component of the centrosome (Lange et al., 2000), where it is involved in the recruitment of other centrosome-associated proteins (Basto et al., 2007; Glover, 2005) and contributes to the proper functioning of the centrosome (de Carcer et al., 2001).

Although the interaction of Hsp90 with MTs is well documented in animal cells, the functional link between these different events has remained obscure. In plants, the interaction of Hsp90 with MTs has been poorly investigated thus far. Searching for MAPs involved in plant growth regulated by light, a heat-stable protein was isolated from maize coleoptiles (Nick et al., 1995). One of these proteins was later identified as a member of the Hsp82/90 family. Hsp90 was found to co-localize with cortical MTs, the preprophase band (PPB) and phragmoplasts in tobacco VBI-0 cells (Petrasek et al., 1998) and was shown to co-assemble with MTs *in vitro* (Freudenreich and Nick, 1998).

Here, we report that plant Hsp90 is enriched in interphasic MT preparations from both non-cycling rice coleoptiles as well as from cycling tobacco BY-2 cells, and is associated with tubulin. Hsp90 binds directly to *in vitro* polymerized MTs and decorates MTs *in vivo*. Overexpression of Hsp90 in BY-2 cells has no phenotypic effect except for a mild decrease in the sensitivity to the tubulin-sequestering compound oryzalin. However, when Hsp90 activity is inhibited by geldanamycin (GDA), the recovery of cortical MTs following cold-induced elimination is impaired, suggesting that Hsp90 is required for the plastic re-organization of plant MTs.

Materials and methods

Plant material

The tobacco cell line BY-2 (*Nicotiana tabacum* L. cv. Bright Yellow 2, BY-2 (Nagata et al., 1992)) and rice seedlings were cultivated as described previously by Jovanovic et al. (2010).

Quantification of mitotic index and response to GDA

Geldanamycin (GDA, Serva) was dissolved in DMSO (stock solution 1.78 mM). GDA was added directly from the stock solution to cultivation medium to reach the final concentration. For long-term GDA treatment, cells were supplemented with 1.78 μM GDA at day 1 after subcultivation and cultivated for an additional 2 days at 26 °C.

To determine the mitotic index, cells at day 1 after subcultivation were supplemented with 178 nM or 1.78 μM GDA, collected 12, 24, 36, and 48 h after GDA addition and fixed in Carnoy fixative (3:1 (v/v) 96% (v/v) ethanol:acetic acid (Campanoni et al., 2003)). Subsequently, they were stained with 2′-(4-hydroxyphenyl)-5-(4-methyl-1-piperazinyl)-2.5′-bi(1H-benzimidazole) trihydrochloride (Hoechst 33258, Sigma–Aldrich, final concentration 1 $\mu g\,mL^{-1}$) and scored under a fluorescence microscope. At least 1200 cells were counted for each sample.

For tests of microtubule (MT) recovery, cells were incubated for 1 h at 0 °C in the presence or absence of 178 nM or 1.78 μM GDA and subsequently transferred to 26 °C for 5 min. After immunofluorescent staining of MTs, more than 100 cells in at least 6 optical fields were counted for fully, partially or no recovered MTs.

Isolation of membrane ghosts

Protoplasts from BY-2 tobacco cell suspension culture were obtained as described by Sonobe and Takahashi (1994). Briefly, the cell wall of 3-day-old BY-2 cells was removed by digestion in 1% cellulase (cellulase "Onozuka" R-10, Yakuruto Honsha Co., Ltd., Japan) and 0.1% pectolyase Y-23 (Kyowa Chemical Products Co., Ltd., Osaka, Japan), supplemented with 0.45 M mannitol, for 3–4.5 h. Protoplasts were overlaid onto the growth medium supplemented with 0.4 M sucrose and centrifuged at 200 × *g* for 10 min. Floating protoplasts were collected, filtered through a nylon mesh (mesh diameter 100 μm), re-suspended in wash buffer [10 mM PIPES (MP Biomedicals, LLC, USA), 100 mM KCl, 285 mM mannitol, pH 6.8], and allowed to attach for 3 min to poly-L-lysine (Sigma–Aldrich, St Louis, MO, USA) coated Petri dishes (diameter 19–19.5 cm) for further protein isolation, or to poly-L-lysine coated coverslips for immunostaining of MTs. Protoplasts were then lysed by incubation for 2 min in lysis buffer (7 mM PIPES, 2 mM EGTA, 10 mM $MgCl_2$, 1% DMSO, 6 mM DTT, 300 μM PMSF, pH 6.9 adjusted with KOH) and a subsequent quick-flick movement. Lysed protoplasts were briefly washed with extraction buffer (25 mM MES, 5 mM EGTA, 5 mM $MgCl_2$, 1 M glycerol, pH 6.9 adjusted with KOH) supplemented with additives (100 μM GTP, 100 μM DDT, 100 μM PMSF, 100 μM Aprotinin, 100 μM Leupeptin, 100 μM Pepstatin) diluted 1:100.

Isolation of proteins from membrane ghosts

Proteins from membrane ghosts were extracted for 1 h with 0.5% CHAPS (MP Biomedicals, Inc., USA) in extraction buffer supplemented with additives in Petri dishes swaying on ice. Proteins were collected, centrifuged at 100 000 × *g* at 4 °C for 30 min, and the supernatant was concentrated using a Vivaspin 4 filtration column (10 000 MWCO, Vivascience, USA).

MT co-sedimentation assay

10 $\mu g\,\mu L^{-1}$ bovine brain tubulin (cat. no. TL238, Cytoskeleton, Inc., USA) in PEM buffer (100 mM PIPES, 1 mM $MgCl_2$, 1 mM EGTA, pH 6.8 adjusted with KOH) was diluted 1:1 with PEMgly (20% (v/v) glycerol in PEM buffer) supplemented with 2 mM GTP and incubated at 35 °C for 20 min. 40 μM taxol and 1 mM GTP in pre-warmed (35 °C) PEM buffer was added and MTs were mixed with membrane ghost-extracted proteins or recombinant NtHsp90_MT, supplemented with 8 μM taxol and the solution was incubated at 28 °C for 1 h. To test the inhibition of its MT-binding activity, the recombinant NtHsp90_MT was supplemented by 1.78 μM GDA and incubated with polymerized tubulin at 37 °C to prevent excessive depolymerization. MTs were overlayed on the 20% sucrose cushion in extraction buffer containing protease inhibitors and sedimented by centrifugation at 100 000 × *g* at 25 °C for 1 h. MTs with bound microtubule-associated proteins (MAPs) in the sediment were precipitated with trichloracetic acid (Bensadoun and Weinstein, 1976), separated on SDS–PAGE acrylamide electrophoresis (Laemmli, 1970) and MALDI analysis was used to identify isolated proteins.

Because some amount of unpolymerized tubulin remained in the sample even after the polymerization step, an additional step, in which unpolymerized tubulin was removed by centrifugation at 100 000 × *g* at 28 °C for 30 min, was added in some cases. The polymerized tubulin found in the pellet was resuspended again in pre-warmed (37 °C) PEM buffer supplemented with 40 μM taxol and 1 mM GTP prior to the incubation with recombinant protein.

Ethyl-N-phenylcarbamate (EPC) affinity chromatography and taxol-induced MT co-sedimentation of MAPs

The EPC affinity chromatography was performed as described by Wiesler et al. (2002). Briefly, carboxy-ethyl-N-phenylcarbamate was synthesized as described by Mizuno et al. (1981), and coupled to sepharose 4B (Amersham-Pharmacia, Freiburg, Germany) that had been extended by an aminoethyl linker (Cuatrecasas, 1970). For soluble protein extraction containing tubulin, the rice coleoptiles were ground by a mortar and pestle in liquid nitrogen. The powder was mixed 1:1 with MT-stabilizing extraction buffer (MSEB: 25 mM MES, 5 mM EGTA, 5 mM $MgCl_2$, 1 M glycerol, 1 mM DTT, 1 mM phenylmethylsulphonyl fluoride, pH 6.9) and centrifuged at 13 000 × *g* for 5 min to remove insoluble tissue debris. After subsequent ultracentrifugation (10 min at 300 000 × *g*, 4 °C; Beckman, USA, TL-100, rotor TLA 100.2), the protein extract was incubated with the same volume of EPC-sepharose pre-equilibrated with MSEB to bind α-tubulin to EPC. Fractions containing proteins bound to α-tubulin were obtained according to Freudenreich and Nick (1998), precipitated with trichloracetic acid (Bensadoun and Weinstein, 1976), separated on SDS–PAGE acrylamide electrophoresis (Laemmli, 1970) and MALDI analysis was used to identify the bound proteins.

The taxol-induced co-sedimentation of MAPs was performed as described by Vantard et al. (1991).

Cloning NtHsp90_MT and OsHsp90_MT for fusion protein expression

mRNA was isolated from 3-day-old BY-2 cells (Qiagen RNAeasy kit, Qiagen, Germany) and followed by RT PCR. Full length cDNA of *NtHsp90_MT* was amplified using primers F5′-GGATCCAATGGCGGAGGCAGAGACG-3′; R5′-AAGCTTTTAGTCAACTTCCTCCATCTT-3′ and inserted into the pDrive cloning vector (Qiagen, Germany). The *Bam*HI–*Xho*I fragment containing full-length *NtHsp90_MT* was cloned into the 0129 pGreen vector, containing *Aph* IV gene providing hygromycin resistance (Hellens et al., 2000), modified by the insertion of *CaMV 35S* promoter, *EGFP* for N-fusion and nopalin synthase (*NOS*) terminator into multi-cloning site (Fischer et al., unpublished). For stable transformation, *Agrobacterium tumefaciens* strain C58C1 carrying the helper plasmid pSoup with a tetracyclin resistance gene (*tet*), and the plant binary vector pGreen0129 were used. The stable transformation was performed as described by Nocarova and Fischer (2009).

Plasmids for stable transformation encoding *GFP-OsHsp90_MT* were constructed via Gateway-based cloning as follows. Primers attB1 5′-GGGGACAAGTTTGTACAAAAAAGCAGGCTTCATGGCCTCG GAGACGGAGACGTTC-3′ and attB2 5′-GGGGACCACTTTGTACAAG AAAGCTGGGTCTTAGTCGACCTCCTCCATCTTGCTC-3′ were used for full length cDNA amplification from rice coleoptiles mRNA, isolated by using Qiagen RNAeasy kit (Qiagen, Germany). Cloning was performed according to Gateway Technology. Stable transformation was performed as described elsewhere (Frey et al., 2009).

Cloning, expression and purification of recombinant *NtHsp90_MT*

For recombinant protein expression, full length *NtHSP90_MT* was amplified using primers flanked by *Sal*I and *Xho*I restriction sites, respectively: F 5′-GTCGACATGGCGGAGGCAGAGACG-3′; R 5′-CTCGAGTTAGTCAACTTCCTCCATCTT-3′, and inserted into the pET28b overexpression vector (Novagen Inc., Darmstadt, Germany) for introduction of the N-terminal polyhistidine tag. Expression of His-NtHsp90_MT was performed as described by Frey et al. (2009).

Phylogenetic analysis and multiple sequence alignment

The evolutionary history was inferred using the Neighbor-Joining method over cytosolic Hsp90s from Solanaceae, *Arabidopsis thaliana*, *Vitis vinifera* and rice (Saitou and Nei, 1987). The bootstrap consensus tree inferred from 500 replicates (Felsenstein, 1985) is taken to represent the evolutionary history of the taxa analyzed (Felsenstein, 1985). Branches corresponding to partitions reproduced in less than 50% of the bootstrap replicates are collapsed. The percentages of replicate trees in which the associated taxa clustered together in the bootstrap test (500 replicates) are shown next to the branches (Felsenstein, 1985). The tree is drawn to scale, with branch lengths in the same units as those of the evolutionary distances used to infer the phylogenetic tree. The evolutionary distances were computed using the Poisson correction method (Zuckerkandl and Pauling, 1965) and are in the units of the number of amino acid substitutions per site. All positions containing gaps and missing data were eliminated from the dataset (Complete deletion option). There were a total of 687 positions in the final dataset. Phylogenetic analyses were conducted in MEGA4 (Tamura et al., 2007).

Visualization of MTs

For immunostaining of MTs in membrane ghosts, poly-L-lysin coated coverslips with membrane ghosts were fixed in 3.7% PFA (Serva, Mannheim, Germany) in MT-stabilizing buffer (MSB, 50 mM PIPES, 2 mM EGTA, 2 mM $MgSO_4$, pH 6.9 adjusted with KOH) for 1 h, washed with MSB 3× 10 min, pre-incubated with 0.5% BSA (MP Biomedicals, Inc., USA) in PBS (NaCl 8 g L^{-1}; KCl 0.2 g L^{-1}; KH_2PO_4 0.158 g L^{-1}; $NaHPO_4{\cdot}12H_2O$ 2.31 g L^{-1}) for 30 min and incubated with monoclonal mouse anti-α-tubulin DM1A (Sigma–Aldrich, St Louis, MO, USA) diluted 1:1000 in PBS for 45 min at RT. After subsequent washing with PBS (3× 10 min), incubation with TRITC-conjugated anti-mouse antibody diluted 1:200 in PBS for 45 min at RT followed. Finally, membrane ghosts were washed (2× 10 min) with PBS, embedded in 50% glycerol in PBS and observed under a confocal scanning microscope.

The immunostaining of MTs in BY-2 cells was performed as described by Schwarzerova et al. (2006) using DM1A as the primary antibody.

Microscopy

The samples were examined on a TCS NT Leica confocal scanning microscope (Leica Microsystems Heidelberg GmbH) using a 63× water immersion objective with 1.2 numerical aperture (HCX PL APO ibd.BL 63.0×/1.2 W), a He/Ne laser for GFP observation (excitation at 488 nm, emission 500–560 nm) and a Ar/Kr laser for TRITC-stained MTs observation (excitation at 543 nm, emission 600–700 nm). Sequential scanning was used for double-stained samples. Image processing was performed using Leica Lite software (Leica Microsystems Heidelberg GmbH).

The samples for mitotic index quantification were examined under an Olympus PROVIS AX 70 fluorescence microscope (Olympus Optical Co., Ltd., Japan) using a 10× objective (UplanApo 10×/0.40) and U-MWU (excitation at 330–385 nm and emission at 420 nm) for mitotic index determination. For observation of cytological changes, the cells were examined in differential interference contrast (DIC) using 20× objective (UplanApo 20×/0.70).

Accession numbers

Sequence data from this article have been deposited at UniProt/GenBank data libraries under accession numbers: A2YWQ1 and HQ834904.

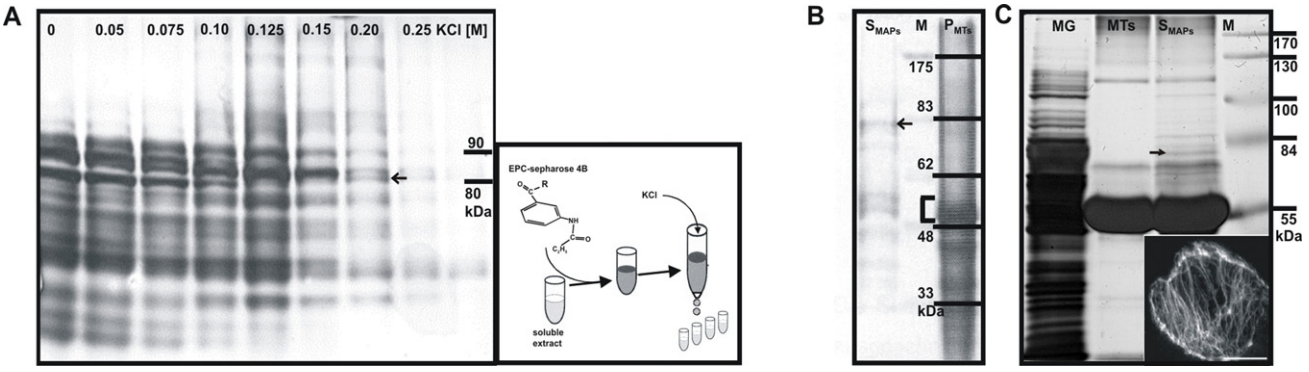

Fig. 1. Isolation of cortical MTs-interacting heat-shock protein 90. (A) Protein profiles of soluble extracts from non-cycling rice coleoptiles eluted with KCl from ethyl-N-phenylcarbamate (EPC) affinity chromatography column. Eluted proteins were separated by SDS–PAGE and stained by Coomassie Blue. An arrow shows the band corresponding to OsHsp90_MT that was identified by MALDI-TOF analysis. The inset shows the principle of the method. (B) Protein profiles of non-cycling rice coleoptiles isolated using microtubule co-sedimentation method. S_{MAPs} – putative MAPs co-assembled with microtubules and detached from the microtubular precipitate (P_{MTs}) by 0.7 M NaCl treatment, the arrow shows OsHsp90_MT (identified by MALDI-TOF analysis). The bracket indicates tubulin, M – size marker. (C) Profiles of proteins solubilized from membrane ghosts from BY-2 cells (MG). Taxol-stabilized MTs before the addition of membrane ghost extract (MTs). Protein profiles solubilized from membrane ghosts and co-sedimented with taxol-stabilized MTs (S_{MAPs}). M – size marker. Hsp90 as MT-interacting protein identified by MALDI-TOF (arrowhead). Inset shows immunofluorescence visualization of cortical microtubules on membrane ghosts. Scale bar: 30 μm.

Results

Hsp90 is co-purified with tubulin from cortical MTs

To gain insight into the role of cortical microtubular arrays, MT-binding proteins from cortical MTs were isolated. To ensure that the cortical MT preparations were not contaminated by mitotic arrays, three different approaches were used. First, cytoskeletal extracts from rice coleoptiles devoid of dividing cells were generated. From these extracts, MAPs were purified either by affinity to α-tubulin-binding herbicide ethyl-N-phenylcarbamate (EPC) (Fig. 1A) or by taxol-induced MT co-sedimentation (Fig. 1B). Second, cortical MTs were separated from mitotic arrays in cycling tobacco BY-2 cells by preparation of membrane ghosts (Fig. 1C, inset). The proteins solubilized by the non-ionic detergent CHAPS from these membrane ghosts were then co-sedimented with MTs (Fig. 1C). The proteins co-purified with cortical MTs through these three approaches were separated by SDS–PAGE and identified by MALDI-TOF.

To identify interesting candidates from non-cycling rice cells, the protein spectra identified from the EPC-affinity approach (Fig. 1A) and the taxol-co-sedimentation approach (Fig. 1B) were compared. Among the number of identified proteins (Supplemental Fig. S1), Hsp81-1 (Swissprot accession A2YWQ1, subsequently termed as OsHsp90_MT) was identified in both protein fractions (Fig. 1A and B, arrowheads).

To identify interesting protein candidates from cycling tobacco BY-2 cells, the protein set interacting with both plasma membrane and MTs was compared to the total protein set extracted from tobacco membrane ghosts (Fig. 1C). Among the MT-specific proteins (Supplemental Fig. S1), the *Nicotiana tabacum* homolog of *N. benthamiana* heat-shock protein 90 (subsequently termed as NtHsp90_MT, see hereafter, NCBI accession HQ834904, Fig. 1C, arrowhead) was identified. Thus, three independent approaches searching for proteins associated with cortical MTs yielded a member of the heat-shock protein 90 family in both the monocot rice as well as in the dicot tobacco. This Hsp90 protein was termed OsHsp90_MT and NtHsp90_MT to specify the particular Hsp90 isoform that was isolated, cloned and expressed in our experiments.

MT-binding Hsp90 harbors a specific KE-rich repeat

Both MT-binding Hsp90 proteins from tobacco and rice harbor characteristic features of cytoplasmic Hsp90 (Fig. 2A). This includes the highly conserved N-terminal ATP-binding pocket that is important for the activation of client proteins (Grenert et al., 1999; Pearl and Prodromou, 2000) and is also a target of the inhibitors GDA and radicicol (Neckers et al., 1999; Pearl and Prodromou, 2000; Prodromou et al., 1997; Sharma et al., 1998; Stebbins et al., 1997). Further, the cytosolic Hsp90 proteins contain the conserved putative casein-kinase II binding motif KEISDDE, the C-terminal MEEVD motif mediating the binding of co-chaperones such as p60 (Krishna and Gloor, 2001; Meyer et al., 2003), and immunophilins (Young et al., 2001), and ten conserved sequence blocks diagnostic for cytosolic Hsp90 species (Krishna and Gloor, 2001). Hsp90s are generally highly conserved and alignments of the two MT-binding Hsp90 proteins with other cytosolic Hsp90 from Solanaceae, *Arabidopsis thaliana*, *Vitis vinifera* and rice revealed about 90% identity (data not shown). When a phylogeny was constructed over these sequences based on a neighbor-joining algorithm (Fig. 2B), the two MT-binding Hsp90 accessions clustered with type II-IV of cytoplasmic Hsp90s following the classification of Krishna and Gloor (2001), whereas lower similarity was found for Hsp90 of type I. The main differences among the Hsp90 proteins were located in two variable stretches that are rich in glutamic-acid residues (the variable KE-rich regions, Fig. 2A and C) and that are thought to mediate rapid interactions with client proteins (Cadepond et al., 1994; Smith, 1993). Both regions contain a charge signature, where positive (K) and negative (E, D) charges follow in several repeats, as shown for the first region (Fig. 2C). Similar KE-containing-repeats have been found to mediate MT-binding in the neural MAP1B (Noble et al., 1989), and have been inferred to mediate the binding of tubulin in the plant MAP AtMAP18 (Wang et al., 2007) and in adenomatous polyposis coli (Deka et al., 1998; Moseley et al., 2007). In these two KE-rich regions, both MT-binding Hsp90 proteins share around 40% identity with AtMAP18 (data not shown), and their similarity with AtMAP18 is higher than with type I Hsp90 proteins (Fig. 2D). However, the prediction of the MT-binding region of Hsp90_MTs is currently based only on alignments and needs to be experimentally verified using truncated proteins.

Purified recombinant Hsp90_MT binds directly to polymerized tubulin in vitro

To test whether NtHsp90_MT can bind to MTs *per se*, the protein was expressed recombinantly as a fusion with a His-tag in *Escherichia coli*, strain BL21(DE3).RIL, using the pET28 vector. The His-tag fusion protein was purified on a Ni-NTA resin column and subsequently analyzed *in vitro* for binding to MTs. After incubation

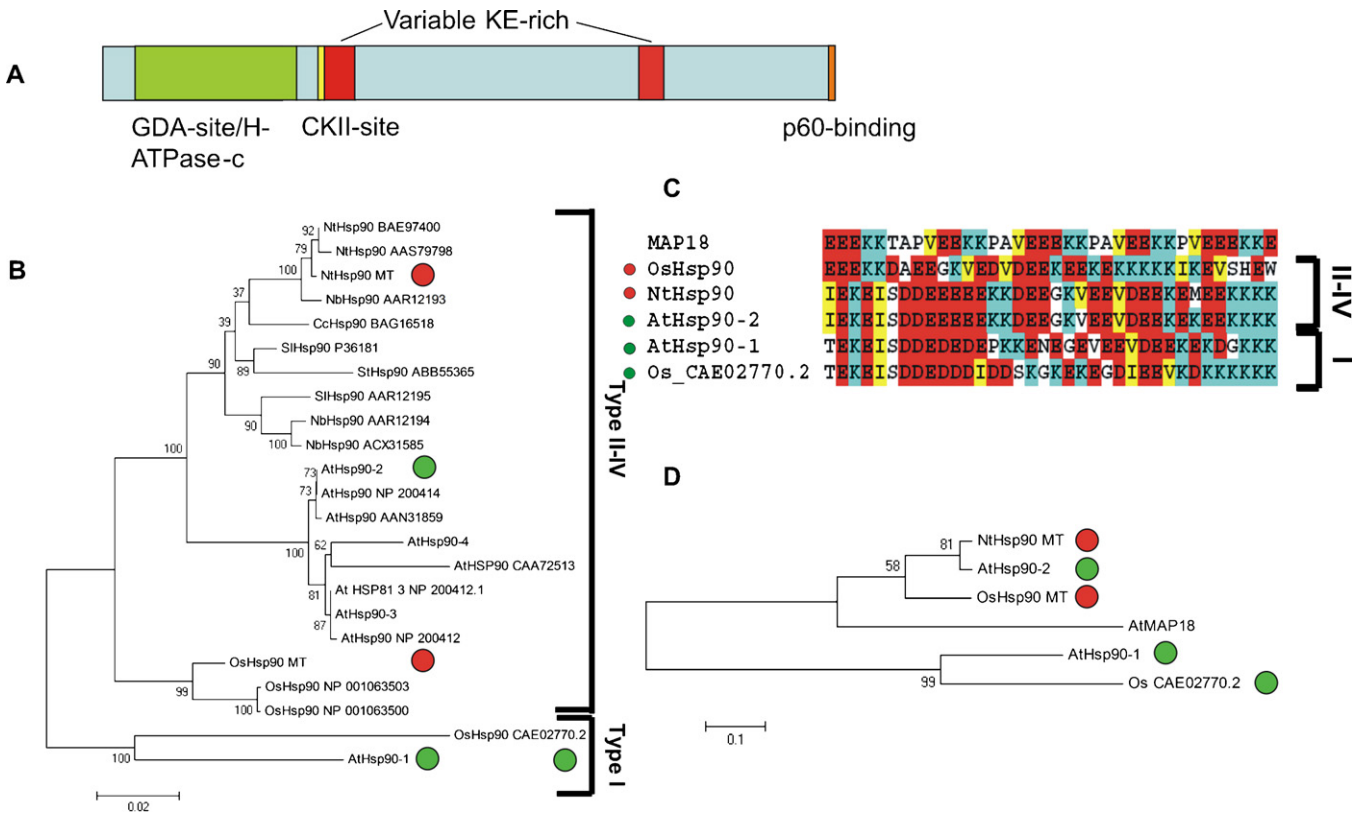

Fig. 2. Microtubule-binding Hsp90s harbor a specific KE-rich repeat. (A) Both tobacco and rice microtubule-binding Hsp90s contain characteristic features described in other cytosolic Hsp90s (for details, see Results): N-terminal ATP and geldanamycin (GDA) binding site (green), putative casein-kinase II (CKII) binding motif KEISDDE (yellow) and C-terminal MEEVD motif mediating the binding of co-chaperones such as p60 (orange). Differences between the different Hsp90 proteins are mainly located in two variable stretches that are rich in K and E amino acid residues (red). (B) A phylogeny constructed over cytosolic Hsp90 sequences shows the clustering of the two microtubule-binding proteins (NtHsp90_MT, OsHsp90_MT, red dots) with type II–IV cytoplasmic Hsp90 and not with the type I Hsp90. Sequences highlighted with green dots were further co-aligned (see (C)). (C) The positive (K) and negative (E) charges in the two variable stretches following in several repeats are shown exemplarily for the first KE-rich region and co-aligned with the microtubule-binding motif of *Arabidopsis* MAP18. (D) In the two KE-rich regions, the similarity of both microtubule-binding Hsp90 proteins with AtMAP18 is higher than with type I Hsp90 proteins. (For interpretation of the references to color in this figure legend, the reader is referred to the web version of the article.)

with polymerized, taxol-stabilized bovine neurotubulin supplemented with BSA as a negative control of MT-binding activity, proteins were co-sedimented through a sucrose cushion. Pelleted MTs (P), the sucrose cushion (C), and the supernatant (S) containing non-polymerized tubulin heterodimers and unbound NtHsp90_MT were separated by SDS–PAGE and visualized by Coomassie Brilliant Blue (Fig. 3A). NtHsp90_MT sedimented in the presence, but not in the absence of MTs (Fig. 3A, P). In contrast, BSA was exclusively found in the soluble fractions (Fig. 3A and C and S), whether MTs were present or not. These data suggest that NtHsp90_MT co-sediments with MTs. A band at 30 kDa apparent molecular weight was observed in these samples, where Hsp90_MT was abundant. MALDI analysis suggested that this band was a product of the recombinant protein partial degradation (data not shown). As Hsp90_MT binds to heterodimeric tubulin (see EPC-affinity chromatography), co-sedimentation with polymerized tubulin may be masked by the presence of higher amounts of unpolymerized tubulin. We therefore repeated the experiment described in Fig. 3A after a supplemental ultracentrifugation step to remove all of the potentially unpolymerized tubulin. The polymerized tubulin from the pellet was resuspended in polymerizing buffer prior the incubation with the recombinant NtHsp90_MT. This variation yielded a significantly higher amount of NtHsp90_MT co-sedimenting with MTs (Fig. 3B, P) when compared to the supernatant (Fig. 3B, S, compare with Fig. 3A), indicating that unpolymerized tubulin can bind to recombinant Hsp90 and mask co-sedimentation with MTs.

As ATP binds to Hsp90 and regulates binding of its client proteins (Pearl and Prodromou, 2000), a potentially similar behavior for tobacco Hsp90_MT was hypothesized. To test whether ATP promotes the MT-binding activity of NtHsp90_MT, a co-sedimentation assay with the addition of ATP was performed. However, the presence of ATP had no effect on the MT-binding activity of NtHsp90_MT (data not shown). Further, we performed the *in vitro* co-sedimentation assay in the presence of GDA (Fig. 3C). Binding to Hsp90_MT ATP-binding domain, GDA did not prevent Hsp90_MT binding to MTs, which is consistent with the previous result, where ATP did not promote the MT-binding activity. The fact that GDA did not interfere with MTs was also suggested in the MT co-sedimentation assay, where cytosolic extract from GFP-Hsp90_MT overexpressing cells was used (Supplemental Fig. S2J). We conclude that another domain, possibly the KE-rich regions, but not the ATP binding domain of Hsp90_MT, is responsible for direct MT-binding.

GFP-Hsp90_MT co-localizes with MTs in vivo and in situ

To test whether Hsp90_MT binds to MTs, tobacco BY-2 cell lines overexpressing fusions between GFP and NtHsp90_MT or OsHsp90_MT were established. The localization of the GFP fusions of NtHsp90_MT (Fig. 4 and Supplemental Fig. S3) and OsHsp90_MT (data not shown) were indistinguishable. As a negative control, a line expressing free GFP was used (Fig. 4B). GFP-Hsp90_MT was found to be localized mainly in the cytoplasm. However, structures resembling microtubular arrays were observed as well. For instance, the Hsp90_MT signal was observed in an equatorial band in cells preparing for mitosis (Supplemental Fig. S3A) reminiscent of a PPB. In metaphase cells, the Hsp90_MT signal was found in

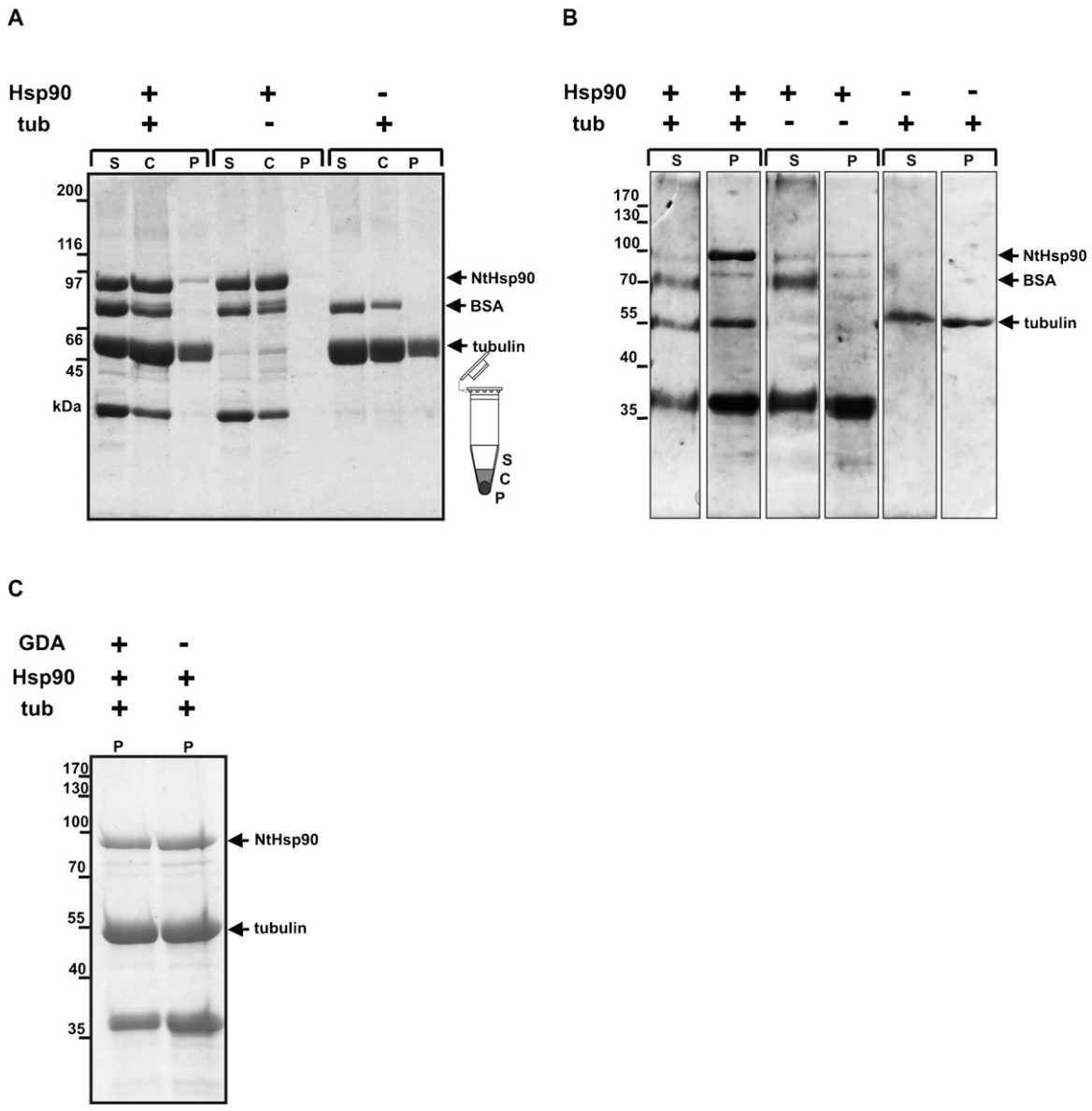

Fig. 3. Purified recombinant Hsp90_MT binds to microtubules *in vitro*. (A) Purified recombinant protein NtHsp90_MT was incubated with taxol-stabilized microtubules, supplemented with BSA as a negative control and centrifuged through a sucrose cushion. The microtubule pellet (P), the sucrose cushion (C), and the supernatant (S) containing tubulin heterodimers and unbound NtHsp90_MT were separated by SDS–PAGE. NtHsp90_MT sedimented in the pellet in the presence of microtubules (P), whereas BSA was exclusively found in the soluble fraction (C and S). (B) The same experiment as described in (A) with an additional centrifugation step of polymerized tubulin in order to remove an excess of unpolymerized tubulin (see Materials and methods for details). An amount of unpolymerized tubulin in the supernatant (S) was decreased. At the same time, more NtHsp90_MT was found in the pellet (P) when co-sedimented with microtubules. The amount of NtHsp90_MT in the pellet was negligible in the absence of microtubules. (C) GDA does not prevent MT-binding activity of Hsp90_MT *in vitro*. Purified recombinant protein NtHsp90_MT was incubated with taxol-stabilized microtubules and GDA to test the inhibition of MT-binding activity. Experiments were performed at 37 °C to prevent MT depolymerization. NtHsp90_MT co-sedimented with microtubules (P) also in the presence of GDA (first lane). Thus, GDA does not prevent Hsp90_MT to bind MTs *in vitro*.

a spindle-like pattern (Supplemental Fig. S3B), and a double-ring that resembled a phragmoplast emerged in telophase cells (Fig. 4A, Supplemental Fig. S3C, and Supplemental movie S5). Whereas free GFP was distributed uniformly in the cell center during telophase (Fig. 4B), the GFP-Hsp90_MT revealed a characteristic interdigitated structure and was confined to a narrower zone along the ensuing cell plate (Fig. 4A, Supplemental Fig. S3C, and Supplemental movie S5).

To test the presumed localization of Hsp90_MT to microtubular structures shown in *in vivo* observations, MTs were immunostained in both GFP-Hsp90_MT expressing lines. GFP-Hsp90_MT was found to be localized in the cytoplasm and it clearly co-localized with MTs in the phragmoplast (Fig. 4C and Supplemental Fig. S2C and S2I). Less prominent but specific localization was observed in PPBs and spindles (Supplemental Fig. S2A, S2B, S2G, and S2H). In contrast, free GFP did not co-localize with MTs in the phragmoplast (Fig. 4D), PPBs and spindles (Supplemental Fig. S2D and S2E). Again, no differences between NtHsp90_MT, (Fig. 4C and Supplemental Fig. S2A–C) and OsHsp90_MT (Supplemental Fig. S2G–I) were detected.

We concluded that Hsp90_MT associates with microtubular structures during cell division, most prominently with the phragmoplast.

GDA affects events requiring MT plasticity

To probe for potential cellular functions of Hsp90–MT-binding, the phenotype of the GFP-NtHsp90_MT and the GFP-OsHsp90_MT overexpressors was carefully analyzed. Viability, rates of cell

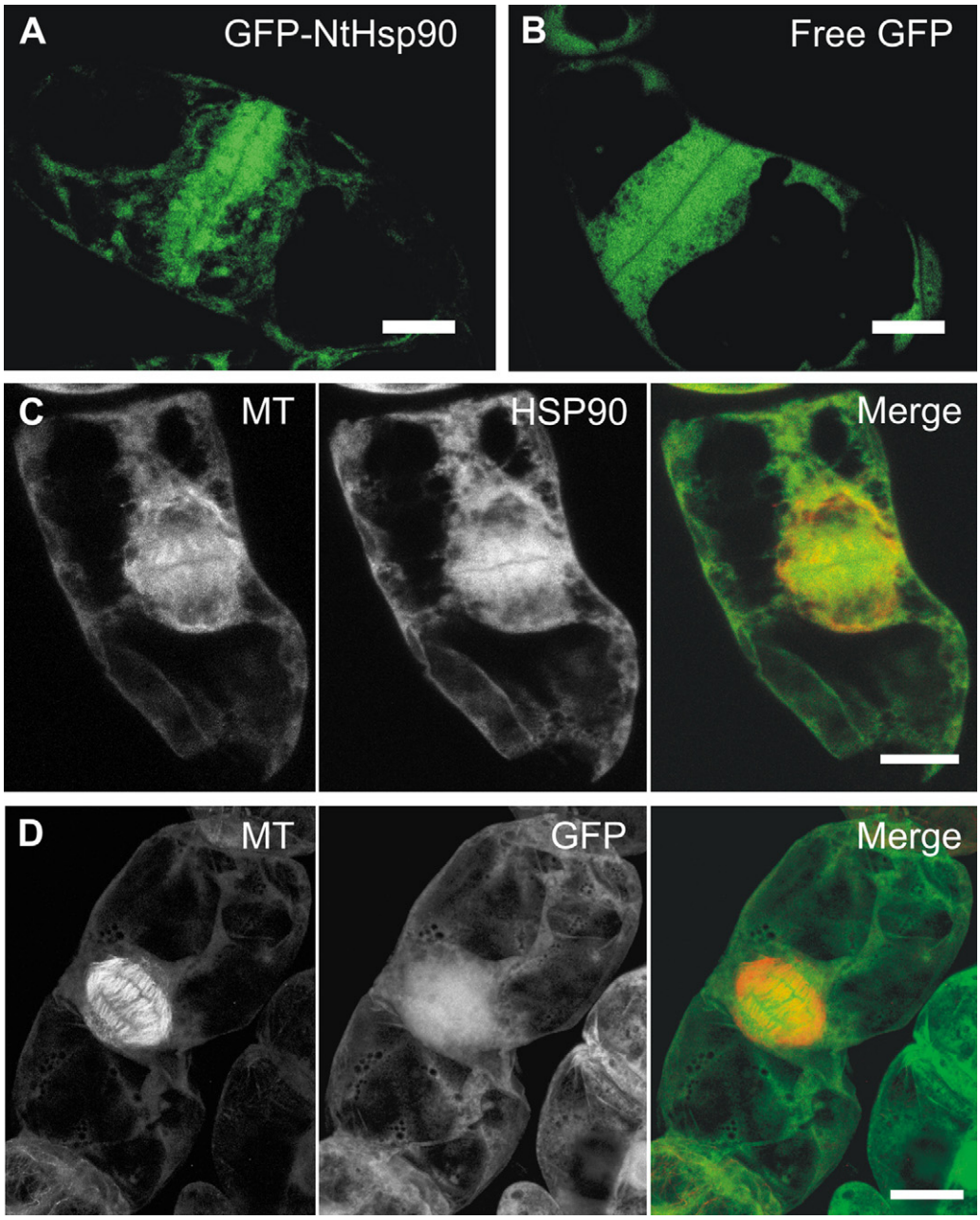

Fig. 4. Localization of Hsp90_MT on microtubules. (A) GFP-NtHsp90_MT in stably expressing tobacco cell line observed under confocal laser scanning microscope. Hsp90_MT was found on microtubular structures of phragmoplast in telophase cells. (B) Free GFP expressing line, a telophase cell with a phragmoplast. GFP was not localized on phragmoplast MTs. Scale bar 20 μm. (C) GFP-NtHsp90_MT-expressing line (green channel) with immunostained MTs (red channel). In telophase cells, GFP-NtHsp90_MT co-localized with phragmoplast MTs. (D) GFP expressing line (green channel) with immunostained MTs (red channel). Phragmoplast MTs in telophase cells were not decorated by GFP. Scale bar 15 μm.

division and cell elongation, and division synchrony (Maisch and Nick, 2007) were not significantly different from non-transformed BY-2 cells or from cells overexpressing free GFP (data not shown). The only difference we were able to trace was a mildly increased resistance to antimicrotubular drugs such as oryzalin and EPC (data not shown), indicating a slightly decreased turnover of MTs. Hsp90 function was pharmacologically inhibited by GDA, a highly specific and broadly used inhibitor of Hsp90 (Whitesell et al., 1994). GDA binds to the ATP-binding pocket, preventing Hsp90 from performing its activity (Prodromou et al., 1997). The response of viability in the two GFP-Hsp90_MT lines using the line overexpressing free GFP and a non-transformed BY-2 (WT) as controls was followed. Neither 0.178 μM GDA nor a ten-fold increased concentration of 1.78 μM GDA induced any decrease in viability over a period of two days (data not shown), indicating that these concentrations within the effect-causing range (Queitsch et al., 2002) do not cause unspecific toxicity. Importantly, mitotic activity was inhibited already during the first 24 h of treatment (Fig. 5O). Within a broad range of GDA concentrations tested, 178 nM GDA was found to inhibit mitosis more severely in control cells, whereas the Hsp90_MT overexpressor showed higher resistance. 1.78 μM GDA, however, blocked mitosis in both of the tested cell lines. This result indicated the importance of Hsp90 in the cell cycle progression and also showed that the elevated concentration of Hsp90 in GFP-NtHsp90_MT overexpressing cell line induced greater resistance of cells to GDA. In order to characterize the effect of GDA on cell

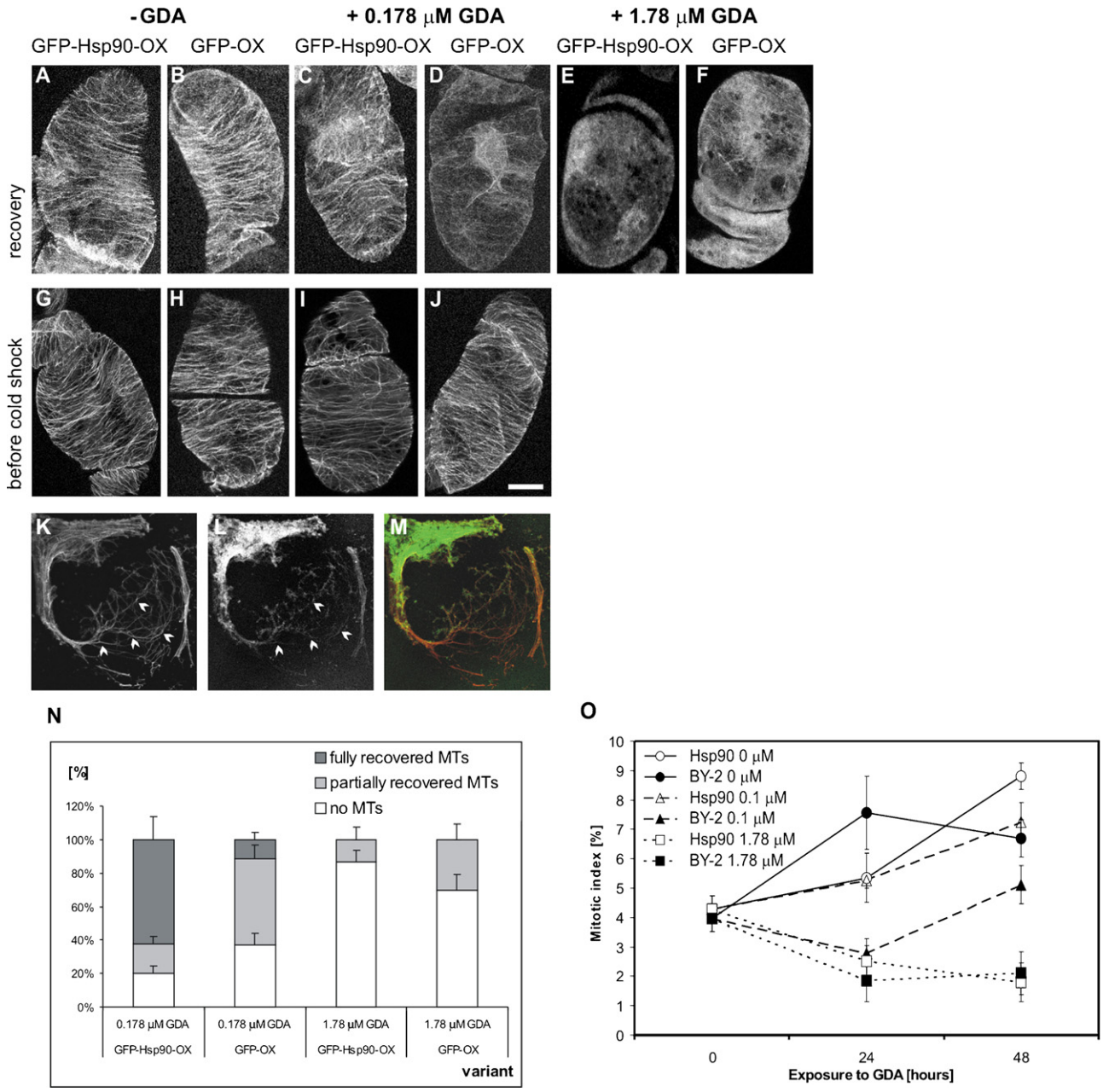

Fig. 5. Events requiring microtubule plasticity are affected during specific Hsp90 inhibition by GDA. (A–J) Geldanamycin impairs the recovery of MTs after cold treatment in tobacco cells. MTs immunostained in GFP-Hsp90_MT or GFP expressing cells are shown (A–J). After 1-h treatment with 0 °C in the presence of 1.78 μM GDA and subsequent recovery at 26 °C for 5 min, both the GFP-Hsp90_MT (E) and free GFP overexpressor (F) showed impaired MT recovery as compared to cells treated with cold in the absence of GDA ((A) for GFP-Hsp90_MT overexpressor, (B) for free GFP overexpressor). GFP-Hsp90_MT overexpressor (C) showed higher resistance to 0,178 μM GDA when compared with GFP overexpressor (D). 1-h treatment of GFP-Hsp90_MT (I) and free GFP expressing cells (J) with 1.78 μM GDA did not cause changes in MT organization when compared to untreated GFP-Hsp90_MT (G) and free GFP (H). Scale bar 15 μm. (K–M) Immunostained cortical MTs (red channel) in membrane ghosts isolated from GFP-Hsp90_MT expressing lines (green channel). GFP-Hsp90_MT (L) decorates cortical MTs (K) (arrows in (L) and (K)). Merge picture (M). Scale bar 30 μm. (N) After the treatment with 0.178 μM GDA, more cells (*y* axis, in percent) with fully recovered MTs were found in GFP-Hsp90_MT overexpressor when compared with GFP overexpressor. In 1.78 μM GDA, no fully recovered MTs were found in both GFP-Hsp90_MT and GFP overexpressor. Error bars = SE, $n = 6–19$. (O) Mitotic activity was inhibited by GDA. 1.78 μM GDA blocked mitosis already within the first 24 h of treatment in both cell lines, whereas non-transformed BY-2 cell line was more sensitive to 100 nM GDA. Hsp90: GFP-Hsp90_MT overexpressing line. Error bars = SE, $n = 6$.

cycle progression, we synchronized BY-2 and GFP-Hsp90_MT overexpressing cells (Supplemental Fig. S4). These results indicated that GDA blocked the cell cycle progression in interphase, between the G1 and S/G2 phases. Further, the flow cytometry of isolated nuclei (using method described in Smetana et al., 2012) from treated and untreated cells was used to specify the phase in which GDA blocks the cell cycle progression. Because the number of cells in the G1 phase increased over S and G2 phase after 24 h of GDA treatment when compared to untreated controls, we concluded that the cells are blocked in G1 (Supplemental Fig. S4).

To probe for MT plasticity in the interphasic cortical array, the influence of GDA on the recovery of cortical MTs after cold shock was tested. Cold treatment efficiently eliminates cortical MTs and some tubulin dimers are then sequestered into the nucleus (Schwarzerova et al., 2006). Upon rewarming, a new cortical array is reorganized from this sequestered tubulin pool within minutes.

When Hsp90 is required for microtubular plasticity, inhibition of Hsp90 activity by GDA is expected to become manifested during this microtubular recovery from cold shock.

In vivo, the localization of Hsp90_MT was relatively cytosolic. Therefore, localization with cortical MTs was tested by isolating membrane ghosts from the GFP-Hsp90_MT overexpressor lines and subsequent visualization of cortical MTs by immunofluorescence. As the inner content of the cell was washed out, the background of cytoplasmic GFP-Hsp90 was reduced such that the observation of the cortical layer became easier. In fact, the GFP signal reporting Hsp90_MT (Fig. 5L) decorating cortical MTs (Fig. 5K) was observed and a merge of the two channels (Fig. 5M) confirmed the association. Thus, Hsp90_MT also binds to cortical MTs. The ability of GFP-Hsp90_MT to interact with MTs was also confirmed using an *in vitro* co-sedimentation assay (Supplemental Fig. S2J). Our results indicated that the GFP tag did not interfere with MT-binding activity of the Hsp90 protein, because it was localized on MTs *in vivo* (Fig. 4A) as well as on MTs in immunostained membrane ghosts (Fig. 5K–M).

After this precondition of a potential function of Hsp90_MT for the plasticity of cortical MTs was demonstrated, the effect of GDA on microtubular recovery from cold-induced de-polymerization in the GFP-NtHsp90_MT overexpressor was tested using the line overexpressing free GFP as a control (Fig. 5A–J). First we examined whether the GDA treatment (1.78 μM, 1 h, RT) *per se* affected cortical MTs, but no differences between untreated cells (Fig. 5G and H) versus GDA-treated cells (Fig. 5I and J) were observed. Second, the cells were kept at 0 °C for 1 h for MT depolymerization and then allowed to recover for 5 min at 26 °C before fixation and immunostaining for MTs. The re-polymerization of MTs was clearly impaired in the presence of GDA (Fig. 5C–F), whereas in the absence of GDA, MTs re-established successfully (Fig. 5A and B). Cells overexpressing GFP-NtHsp90_MT, however, showed greater resistance to GDA (Fig. 5C). These cells re-polymerized MTs faster in the presence of 178 nM GDA when compared to GFP overexpressor (Fig. 5D), because significantly more cells showed fully polymerized MTs after the recovery period (Fig. 5N). This indicated that the overexpression of Hsp90_MT rendered MTs less susceptible to GDA, probably due to greater amounts of functional Hsp90 assisting in MT re-polymerization in cells treated with 178 nM GDA. In accordance with this idea, a high concentration of GDA (1.78 μM) prevented MTs recovery after cold shock in both GFP-NtHsp90_MT (Fig. 5E) and GFP overexpressing cells (Fig. 5F). Despite the impaired recovery within the first minutes in the presence of 1.78 μM GDA, MTs were fully re-polymerized after 1 h (data not shown) and the GDA treatment did not affect viability over the subsequent days (data not shown). Nevertheless, our results indicated that the inhibition of Hsp90 using GDA affected early phases of rapid MTs re-polymerization.

Discussion

In the last decades, Hsp90 has been shown to associate with MTs in several studies. Similar to previous experiments (Freudenreich and Nick, 1998), plant Hsp90 was co-purified with both polymerized MTs and with soluble tubulin heterodimers in our study. However, since cytosolic extracts were used, these approaches did not reveal whether the interaction of Hsp90 with tubulin is direct or mediated by other proteins. Similarly, evidence based on immunofluorescence co-localization of plant Hsp90 with MTs (Petrasek et al., 1998) cannot discriminate between direct and indirect MT-binding of Hsp90. An additional problem with antibody-based approaches is highly probable cross-reactions with different members of the Hsp90 gene family. In the current work, we took advantage of the use of one specific plant Hsp90 associated with MTs (termed as NtHsp90_MT and OsHsp90_MT) fused to GFP. The association was clearly demonstrated for phragmoplast MTs as well as for cortical MTs in membrane ghosts. Since the GFP-tagged protein also cannot discriminate between direct and indirect MT-binding, we used the recombinant tobacco Hsp90_MT for the co-sedimentation with polymerized MTs *in vitro* in the absence of other cytosolic proteins. This provides evidence that the Hsp90_MT-MT interaction is direct. Since the addition of ATP did not cause any changes in the binding of Hsp90_MT to MTs in the *in vitro* co-sedimentation assay, the process is either ATP-independent, as suggested previously (Jakob et al., 1995), or, as proposed by Marcu et al. (2000), the GTP from the solution is utilized. Further, GDA did not prevent the Hsp90_MT MT-binding activity *in vitro*. Both of these results show that the ATP-binding pocket is not the domain involved in the interaction between Hsp90 and MTs. The protein domain responsible for direct Hsp90–MTs interaction remains to be characterized.

Studies of animal Hsp90 have been based on experiments using cellular extracts and antibodies that did not discriminate between different specific Hsp90s. The homologs of Hsp90 were observed to associate with MTs in cilia and cortex of *Tetrahymena* cells (Williams and Nelsen, 1997). In human cells, Hsp90 was recruited preferentially on MTs containing acetylated tubulin (Giustiniani et al., 2009). As a part of heterocomplex with client proteins and immunophilin, Hsp90 is linked to dynein, the motor protein for retrograde movement along MTs toward the nucleus (Galigniana et al., 2004; Harrell et al., 2004; Pratt et al., 2004). Further, Hsp90 was reported to localize in *Drosophila* centrosomes (Lange et al., 2000), and to be involved in the γ-tubulin ring assembly (Glover, 2005). With respect to these multiple MT-targeted functions of animal Hsp90, the Hsp90 interactions with plant MTs reported in our study are likely to be accompanied by additional functions as well. Moreover, the association of plant Hsp90_MT with MTs is transient, of short duration and rather weak, which is indicated by the fact that the Hsp90_MT signal on cortical MTs was manifested in membrane ghosts, but was obscured in living cells. A similar short and transient association of highly dynamic heterocomplexes mediated by Hsp90 was also detected in mammalian cells (Pratt et al., 1999). Interestingly, the ratio between Hsp90_MT co-sedimented with MTs and that remaining in the supernatant can be shifted in favor of MT co-sedimented recombinant protein, if unpolymerized tubulin is removed from the reaction in an *in vitro* co-sedimentation assay. Again, this indicates the ability of Hsp90_MT to bind soluble tubulin heterodimers as well, as also suggested by our EPC-affinity assay. Indeed, Hsp90 interacts with tubulin dimers in animal cells (Sanchez et al., 1988; Weis et al., 2010). This putative binding of the GFP-Hsp90_MT to tubulin heterodimers may hamper the observation of GFP-Hsp90_MT in living cells. Nevertheless, it will be very interesting to characterize functions of Hsp90_MT bound to tubulin dimers or to MTs.

We failed to observe any striking phenotype in lines that overexpressed GFP-Hsp90_MT, with the exception of a slight decrease in turn-over of MTs deduced from a small reduction in sensitivity to the tubulin-sequestering drug oryzalin. Therefore, the specific Hsp90 inhibitor GDA that binds to the ATP-binding pocket of Hsp90, thus preventing the subsequent activation of Hsp90 client proteins (Grenert et al., 1999; Prodromou et al., 1997), was used to identify MT-driven functions of Hsp90s. We focused on events in which MTs exhibit their plasticity, i.e. where the whole microtubular network undergoes extensive remodeling. The re-constitution of cortical MTs after their cold-induced de-polymerization (Pokorna et al., 2004; Schwarzerova et al., 2006) represents such a situation. Since Hsp90_MT in fusion with GFP was found to decorate immunolabeled cortical MTs in membrane ghosts, recovery of cortical MTs after cold treatment appeared to be a promising candidate. In fact, the GDA-treated cells did not restore MTs properly. At room

temperature, the same concentration of GDA had no effect on MTs in control cells, indicating that Hsp90 is not required for MT organization *per se*, but becomes limiting under conditions of rapid re-modeling. The fact that GDA as a specific inhibitor of Hsp90 affected MTs re-organization and that Hsp90_MT overexpressing cells reconstituted MTs in the presence of GDA faster than control cells indicated that Hsp90_MT was indeed required for the plasticity of MTs. This conclusion is also supported by our finding that Hsp90 is concentrated on phragmoplast MTs, where high MT growth and assembly is required. However, the molecular mechanism of this feature remains to be elucidated. Our results indicated that GDA does not prevent Hsp90_MT from direct binding to MTs *in vitro*. The interaction of Hsp90_MT with MTs might therefore be modulated by other client and interacting proteins (for review, see Wegele et al., 2004), whose binding to Hsp90_MT is affected by GDA binding to the ATP pocket. The search for these interaction factors will be a primary goal in our future studies.

A similar role of Hsp90 in MT plasticity has also been reported for *Drosophila*, where Hsp90 was reported as a core centrosomal component (Lange et al., 2000). Here, MTs in interphase cultured animal cells were not affected by GDA treatment. However, spindles of mitotic cells were found to be aberrant due to abnormal centrosomes formed in treated cells (Lange et al., 2000). Salt-stripped *Drosophila* centrosomes failed to re-establish MT-nucleating activity after GDA treatment (de Carcer et al., 2001). It has also become clear that MT nucleation requires additional Hsp90-interacting centrosomal proteins in animal cells, such as Polo kinase in *Drosophila* (de Carcer, 2004; Glover, 2005) and Hsp90 is required to recruit Msps, a homolog of XMAP215/chTOG in *Drosophila*, and cyclin B to centrosome in *Drosophila* and human cells (Basto et al., 2007). Our results indicate that Hsp90_MT may also play an important role in MT-nucleation sites in acentrosomal plant cells, where nucleation of MTs seems to occur from dispersed sites (Murata et al., 2005). It is also likely that in acentrosomal cells, Hsp90 is acting in concert with other MT-nucleating proteins. Therefore, further studies on the role of Hsp90 in MT-nucleation in acentrosomal plant cells and further characterization of interacting proteins might lead to better understanding of plant MT-nucleation molecular mechanism. Our experiments with the Hsp90 inhibitor GDA suggested that Hsp90 also plays role in the cell cycle progression. In non-plant cells, downstream effects of Hsp90 inhibition include also cell cycle arrest in various stages of the cell cycle, where molecular mechanisms of these effects probably differ depending on the cell type (Zajac et al., 2008). Although it is likely that the role of Hsp90 in the regulation of the cell cycle is widespread in eukaryotic cells, the exact molecular mechanism of the effect of Hsp90 inhibition on the mitosis inhibition in tobacco cells needs further investigation. Our results suggest that BY-2 cells are blocked in the G1 phase. Therefore, GDA blocks the cell cycle progression before mitotic array assembly in tobacco cells. It remains to be established whether the MT-binding function of Hsp90 and the cell cycle progression block are related or independent processes controlled by Hsp90.

The involvement of Hsp90_MT in MT remodeling might also contribute to the role of Hsp90 as the morphogenetic capacitor described for *A. thaliana* (Queitsch et al., 2002). Since re-orientations of cortical MTs precede and control the axis of cell expansion via the orientation of cellulose synthesis (Paredez et al., 2006), Hsp90_MTs are expected, under environmental constraints, to act as limiting factors for plant morphogenesis. Therefore, the link between phenotypic capacity and Hsp90_MT might be revealing.

Functional assignment is straightforward in cases where a protein performs a unique task, such as catalyzing a step in a metabolic pathway. Proteins that are ubiquitous and interact with a large number of partners are more difficult to analyze, because loss- and gain-of-function assays produce pleiotropic effects. This often leads to the impression that these proteins do not perform any specific function. However, it might be that these, at first sight not very specific, proteins, are crucial for developmental and evolutionary plasticity. By their multiple interactions, these proteins are pacemakers for new interaction networks (Uhrig, 2006). In addition to their primary function, these proteins can fulfill several "moonlighting" tasks that can evolve into a new main function in a different functional context (Kurakin, 2005). Our central finding that Hsp90_MT, as a relatively ubiquitous protein, will exert specific effects under conditions of environmental constraints (microtubular recovery from cold stress) would be consistent with its role as phenotypic capacitor (Queitsch et al., 2002).

Acknowledgments

We thank Jan Petrášek and Lukáš Fischer for stimulating discussions and continuous interest in the project. We also thank Dimitri Heintz for MALDI-TOF analysis, Ondřej Smetana for flow cytometry experiments and Nicole Frey for help with the protein extraction and valuable suggestions.

The work was supported by the grant of the Ministry of Education, Youth and Sports of the Czech Republic [grant numbers ME10111, LC06034 and MSM 0021620858], the Czech-German DAAD project [D14-CZ 14/2008-09] and by the grants of Charles University in Prague GAUK [grant number 82710/2010] and SVV 265203/2012.

Appendix A. Supplementary data

Supplementary data associated with this article can be found, in the online version, at http://dx.doi.org/10.1016/j.jplph.2012.06.010.

References

Akhmanova A, Steinmetz MO. Tracking the ends: a dynamic protein network controls the fate of microtubule tips. Nat Rev Mol Cell Biol 2008;9:309–22.

Basto R, Gergely F, Draviam VM, Ohkura H, Liley K, Raff JW. Hsp90 is required to localise cyclin B and Msps/ch-TOG to the mitotic spindle in *Drosophila* and humans. J Cell Sci 2007;120:1278–87.

Bensadoun A, Weinstein D. Assay of proteins in presence of interfering materials. Anal Biochem 1976;70:241–50.

Boter M, Amigues B, Peart J, Breuer C, Kadota Y, Casais C, et al. Structural and functional analysis of SGT1 reveals that its interaction with HSP90 is required for the accumulation of Rx, an R protein involved in plant immunity. Plant Cell 2007;19:3791–804.

Cadepond F, Jibard N, Binart N, Schweizergroyer G, Segardmaurel I, Baulieu EE. Selective deletions in the 90 kDa heat-shock protein (HSP90) impede heterooligomeric complex formation with glucocorticosteroid receptor (GR) or hormone-binding by GR. J Steroid Biochem Mol Biol 1994;48:361–7.

Campanoni P, Blasius B, Nick P. Auxin transport synchronizes the pattern of cell division in a tobacco cell line. Plant Physiol 2003;133:1251–60.

Cuatrecasas P. Protein purification by affinity chromatography – derivatizations of agarose and polyacrylamide beads. J Biol Chem 1970;245:3059–65.

de Carcer G. Heat shock protein 90 regulates the metaphase-anaphase transition in a polo-like kinase-dependent manner. Cancer Res 2004;64:5106–12.

de Carcer G, Avides MD, Lallena MJ, Glover DM, Gonzalez C. Requirement of Hsp90 for centrosomal function reflects its regulation of Polo kinase stability. EMBO J 2001;20:2878–84.

Deeks MJ, Fendrych M, Smertenko A, Bell KS, Oparka K, Cvrckova F, et al. The plant formin AtFH4 interacts with both actin and microtubules, and contains a newly identified microtubule-binding domain. J Cell Sci 2010;123:1209–15.

Deka J, Kuhlmann J, Muller O. A domain within the tumor suppressor protein APC shows very similar biochemical properties as the microtubule-associated protein tau. Eur J Biochem 1998;253:591–7.

Felsenstein J. Confidence-limits on phylogenies – an approach using the bootstrap. Evolution 1985;39:783–91.

Fostinis Y, Theodoropoulos PA, Gravanis A, Stournaras C. Heat-shock protein HSP90 and its association with the cytoskeleton – a morphological study. Biochem Cell Biol 1992;70:779–86.

Freudenreich A, Nick P. Microtubular organization in tobacco cells: heat-shock protein 90 can bind to tubulin in vitro. Bot Acta 1998;111:273–9.

Frey N, Klotz J, Nick P. Dynamic bridges – a calponin-domain kinesin from rice links actin filaments and microtubules in both cycling and non-cycling cells. Plant Cell Physiol 2009;50:1493–506.
Galigniana MD, Harrell JM, O'Hagen HM, Ljungman M, Pratt WB. Hsp90-binding immunophilins link p53 to dynein during p53 transport to the nucleus. J Biol Chem 2004;279:22483–9.
Gardiner JC, Harper JDI, Weerakoon ND, Collings DA, Ritchie S, Gilroy S, et al. A 90-kD phospholipase D from tobacco binds to microtubules and the plasma membrane. Plant Cell 2001;13:2143–58.
Giustiniani J, Daire V, Cantaloube I, Durand G, Pous C, Perdiz D, et al. Tubulin acetylation favors Hsp90 recruitment to microtubules and stimulates the signaling function of the Hsp90 clients Akt/PKB and p53. Cell Signal 2009;21:529–39.
Glover DM. Polo kinase and progression through M phase in *Drosophila*: a perspective from the spindle poles. Oncogene 2005;24:230–7.
Grenert JP, Johnson BD, Toft DO. The importance of ATP binding and hydrolysis by hsp90 in formation and function of protein heterocomplexes. J Biol Chem 1999;274:17525–33.
Hamada T. Microtubule-associated proteins in higher plants. J Plant Res 2007;120:79–98.
Harrell JM, Kurek I, Breiman A, Radanyi C, Renoir JM, Pratt WB, et al. All of the protein interactions that link steroid receptor center dot hsp90 center dot immunophilin heterocomplexes to cytoplasmic dynein are common to plant and animal cells. Biochemistry 2002;41:5581–7.
Harrell JM, Murphy PJM, Morishima Y, Chen HF, Mansfield JF, Galigniana MD, et al. Evidence for glucocorticoid receptor transport on microtubules by dynein. J Biol Chem 2004;279:54647–54.
Hellens RP, Edwards EA, Leyland NR, Bean S, Mullineaux PM. pGreen: a versatile and flexible binary Ti vector for *Agrobacterium*-mediated plant transformation. Plant Mol Biol 2000;42:819–32.
Jakob U, Lilie H, Meyer I, Buchner J. Transient interaction of HSP90 with early unfolding intermediates of citrate synthase – implications for heat shock *in vivo*. J Biol Chem 1995;270:7288–94.
Jovanovic AM, Durst S, Nick P. Plant cell division is specifically affected by nitrotyrosine. J Exp Bot 2010;61:901–9.
Koyasu S, Nishida E, Kadowaki T, Matsuzaki F, Iida K, Harada F, et al. 2 mammalian heat-shock proteins HSP90 and HSP100, are actin-binding proteins. Cell Struct Funct 1986;11:440–1.
Krishna P, Gloor G. The Hsp90 family of proteins in *Arabidopsis thaliana*. Cell Stress Chaperones 2001;6:238–46.
Kurakin A. Self-organization versus Watchmaker: stochastic dynamics of cellular organization. Biol Chem 2005;386:247–54.
Laemmli UK. Cleavage of structural proteins during assembly of head of bacteriophage-T4. Nature 1970;227:680–5.
Lange BMH, Bachi A, Wilm M, Gonzalez C. Hsp90 is a core centrosomal component and is required at different stages of the centrosome cycle in *Drosophila* and vertebrates. EMBO J 2000;19:1252–62.
Lloyd C, Chan J. Microtubules and the shape of plants to come. Nat Rev Mol Cell Biol 2004;5:13–22.
Maisch J, Nick P. Actin is involved in auxin-dependent patterning. Plant Physiol 2007;143:1695–704.
Marcu MG, Chadli A, Bouhouche I, Catelli M, Neckers LM. The heat shock protein 90 antagonist novobiocin interacts with a previously unrecognized ATP-binding domain in the carboxyl terminus of the chaperone. J Biol Chem 2000;275:37181–6.
Meyer P, Prodromou C, Hu B, Vaughan C, Roe SM, Panaretou B, et al. Structural and functional analysis of the middle segment of Hsp90: implications for ATP hydrolysis and client protein and cochaperone interactions. Mol Cell 2003;11:647–58.
Mizuno K, Koyama M, Shibaoka H. Isolation of plant tubulin from azuki bean epicotyls by ethyl N-phenylcarbamate-sepharose affinity-chromatography. J Biochem 1981;89:329–32.
Moseley JB, Bartolini F, Okada K, Wen Y, Gundersen GG, Goode BL. Regulated binding of adenomatous polyposis coli protein to actin. J Biol Chem 2007;282:12661–8.
Murata T, Sonobe S, Baskin TI, Hyodo S, Hasezawa S, Nagata T, et al. Microtubule-dependent microtubule nucleation based on recruitment of gamma-tubulin in higher plants. Nat Cell Biol 2005;7:961–8.
Nagata T, Nemoto Y, Hasezawa S. Tobacco BY-2 cell line is the "HeLa" cell in the cell biology of higher plants. Int Rev Cytol Surv Cell Biol 1992;132:1–30.
Neckers L, Schulte TW, Mimnaugh E. Geldanamycin as a potential anti-cancer agent: its molecular target and biochemical activity. Invest New Drugs 1999;17:361–73.
Nick P, Heuing A, Ehmann B. Plant chaperonins: a role in microtubule-dependent wall formation? Protoplasma 2000;211:234–44.
Nick P, Lambert AM, Vantard M. A microtubule-associated protein in maize is expressed during phytochrome-induced cell elongation. Plant J 1995;8:835–44.
Noble M, Lewis SA, Cowan NJ. The microtubule binding domain of microtubule-associated protein MAP1B contains a repeated sequence motif unrelated to that of MAP2 and tau. J Cell Biol 1989;109:3367–76.
Nocarova E, Fischer L. Cloning of transgenic tobacco BY-2 cells; an efficient method to analyse and reduce high natural heterogeneity of transgene expression. BMC Plant Biol 2009;9:44.
Paredez AR, Somerville CR, Ehrhardt DW. Visualization of cellulose synthase demonstrates functional association with microtubules. Science 2006;312:1491–5.
Pearl LH, Prodromou C. Structure and in vivo function of Hsp90. Curr Opin Struct Biol 2000;10:46–51.
Petrasek J, Freudenreich A, Heuing A, Opatrny Z, Nick P. Heat-shock protein 90 is associated with microtubules in tobacco cells. Protoplasma 1998;202:161–74.
Pokorna J, Schwarzerova K, Zelenkova S, Petrasek J, Janotova I, Capkova V, et al. Sites of actin filament initiation and reorganization in cold-treated tobacco cells. Plant Cell Environ 2004;27:641–53.
Pratt WB, Galigniana MD, Harrell JM, DeFranco DB. Role of hsp90 and the hsp90-binding immunophilins in signalling protein movement. Cell Signal 2004;16:857–72.
Pratt WB, Silverstein AM, Galigniana MD. A model for the cytoplasmic trafficking of signalling proteins involving the hsp90-binding immunophilins and p50(cdc37). Cell Signal 1999;11:839–51.
Prodromou C, Roe SM, Obrien R, Ladbury JE, Piper PW, Pearl LH. Identification and structural characterization of the ATP/ADP-binding site in the Hsp90 molecular chaperone. Cell 1997;90:65–75.
Queitsch C, Sangster TA, Lindquist S. Hsp90 as a capacitor of phenotypic variation. Nature 2002;417:618–24.
Rutherford SL, Lindquist S. Hsp90 as a capacitor for morphological evolution. Nature 1998;396:336–42.
Rutherford SL, Zuker CS. Protein folding and the regulation of signaling pathways. Cell 1994;79:1129–32.
Saitou N, Nei M. The neighbor-joining method – a new method for reconstructing phylogenetic trees. Mol Biol Evol 1987;4:406–25.
Sanchez ER, Redmond T, Scherrer LC, Bresnick EH, Welsh MJ, Pratt WB. Evidence that the 90-kilodalton heat shock protein is associated with tubulin-containing complexes in L cell cytosol and in intact PtK cells. Mol Endocrinol 1988;2:756–60.
Schwarzerova K, Petrasek J, Panigrahi KCS, Zelenkova S, Opatrny Z, Nick P. Intranuclear accumulation of plant tubulin in response to low temperature. Protoplasma 2006;227:185–96.
Sharma SV, Agatsuma T, Nakano H. Targeting of the protein chaperone HSP90, by the transformation suppressing agent, radicicol. Oncogene 1998;16:2639–45.
Smetana O, Široký J, Houlné G, Opatrný Z, Chabouté ME. Non-apoptotic programmed cell death with paraptotic-like features in bleomycin-treated plant cells is suppressed by inhibition of ATM/ATR pathways or NtE2F overexpression. J Exp Bot 2012;63:2631–44.
Smith DF. Dynamics of heat-shock protein 90-progesterone receptor binding and the disactivation loop model for steroid receptor complexes. Mol Endocrinol 1993;7:1418–29.
Sonobe S, Takahashi S. Association of microtubules with the plasma membrane of tobacco BY-2 cells *in vitro*. Plant Cell Physiol 1994;35:451–60.
Stebbins CE, Russo AA, Schneider C, Rosen N, Hartl FU, Pavletich NP. Crystal structure of an Hsp90–geldanamycin complex: targeting of a protein chaperone by an antitumor agent. Cell 1997;89:239–50.
Stoppin-Mellet V, Gaillard J, Timmers T, Neumann E, Conway J, Vantard M. *Arabidopsis* katanin binds microtubules using a multimeric microtubule-binding domain. Plant Physiol Biochem 2007;45:867–77.
Takabatake R, Ando Y, Seo S, Katou S, Tsuda S, Ohashi Y, et al. MAP kinases function downstream of HSP90 and upstream of mitochondria in TMV resistance gene N-mediated hypersensitive cell death. Plant Cell Physiol 2007;48:498–510.
Takahashi A, Casais C, Ichimura K, Shirasu K. HSP90 interacts with RAR1 and SGT1 and is essential for RPS2-mediated disease resistance in *Arabidopsis*. Proc Natl Acad Sci USA 2003;100:11777–82.
Tamura K, Dudley J, Nei M, Kumar S. MEGA4: molecular evolutionary genetics analysis (MEGA) software version 4.0. Mol Biol Evol 2007;24:1596–9.
Uhrig JF. Protein interaction networks in plants. Planta 2006;224:771–81.
Vantard M, Schellenbaum P, Fellous A, Lambert AM. Characterization of maize microtubule-associated proteins, one of which is immunologically related to tau. Biochemistry 1991;30:9334–40.
Wang X, Zhu L, Liu BQ, Wang C, Jin LF, Zhao Q, et al. *Arabidopsis* MICROTUBULE-ASSOCIATED PROTEIN18 functions in directional cell growth by destabilizing cortical microtubules. Plant Cell 2007;19:877–89.
Wegele H, Muller L, Buchner J. Hsp70 and Hsp90 – a relay team for protein folding. Rev Physiol Biochem Pharmacol 2004;151:1–44.
Weis F, Moullintraffort L, Heichette C, Chretien D, Garnier C. The 90-kDa heat shock protein Hsp90 protects tubulin against thermal denaturation. J Biol Chem 2010;285:9525–34.
Whitesell L, Mimnaugh EG, Decosta B, Myers CE, Neckers LM. Inhibition of heat-shock protein HSP90-PP60(V-SRC) heteroprotein complex formation by benzoquinone ansamycins – essential role for stress proteins in oncogenic transformation. Proc Natl Acad Sci USA 1994;91:8324–8.
Wiesler B, Wang QY, Nick P. The stability of cortical microtubules depends on their orientation. Plant J 2002;32:1023–32.
Williams NE, Nelsen EM. HSP70 and HSP90 homologs are associated with tubulin in hetero-oligomeric complexes, cilia and the cortex of *Tetrahymena*. J Cell Sci 1997;110:1665–72.
Young JC, Moarefi I, Hartl FU. Hsp90: a specialized but essential protein-folding tool. J Cell Biol 2001;154:267–73.
Zajac M, Moneo MV, Carnero A, Benitez J, Martinez-Delgado B. Mitotic catastrophe cell death induced by heat shock protein 90 inhibitor in BRCA1-deficient breast cancer cell lines. Mol Cancer Ther 2008;7:2358–66.
Zuckerkandl E, Pauling L. Evolutionary divergence and convergence in proteins. In: Bryson V, Vogel HJ, editors. Evolving genes and proteins. New York: Academic Press; 1965. p. 99–166.